Geomechanics and Engineering, *Vol. 34, No. 5 (2023) 481-489*
https://doi.org/10.12989/gae.2023.34.5.481

The drained deformation characteristics of sand subjected to lateral cyclic loading

Junhua Xiao[1,2a], Jiapei Ma[1,2b], Jianfeng Xue[3c], Zhiyong Liu*[1,2] and Yingqi Bai[1,2d]

[1]*Shanghai Key Laboratory of Rail Infrastructure Durability and System Safety, Tongji University, Shanghai, 201804, China*
[2]*Key Laboratory of Road and Traffic Engineering of Ministry of Education, Tongji University, Shanghai, 201804, China*
[3]*School of Engineering and Information Technology, University of New South Wales, Campbell, ACT, 2612, Australia*

(*Received May 7, 2023, Revised July 4, 2023, Accepted July 14, 2023*)

Abstract. Drained cyclic triaxial tests were conducted on a saturated sand to examine its deformation characteristics under either axial or lateral cyclic loading condition. To apply lateral cyclic loading, the cell pressure was cycled while maintaining a constant vertical stress. The strain accumulations and flow direction in the soil were presented and discussed considering various initial stress ratios (η_0), cyclic stress amplitudes and cyclic stress paths. The results indicate that axial strain accumulation shows an exponential increase with the maximum stress ratio (η^{max}). The initial deviatoric stress has comparable effects with lateral cyclic stress amplitude on the accumulated axial strain. In contrast, the accumulated volumetric strain is directly proportional to the lateral cyclic stress amplitude but not much affected by η_0 values. Due to the anisotropy of the soil, the accumulated axial and lateral bulging strains are greater in lateral cyclic loading when compared to axial cyclic loading even though η^{max} is the same. It is also found that η^{max} affects soil's lateral deformation and increasing the ratio could change the lateral deformation from contraction to bulging. The flow direction depends on η^{max} in the sand under lateral cyclic loading, regardless of η_0 values and the cyclic stress amplitudes, and a large η^{max} could lead to great deviatoric strain but a little volumetric strain accumulation.

Keywords: lateral cyclic loading; saturated sand; strain accumulation; strain accumulation direction

1. Introduction

Lateral cyclic loading, for instance, tide, wave and wind loading, leads to accumulative deformation in the surrounding soils, which threatens the safety and serviceability of geotechnical structures (Liu and Xue 2022). Studying soil's deformation characteristics under lateral cyclic loading condition is crucial to foresee the long-term deformation of such structures and achieve a safe and economic design in engineering practice.

The deformation of geotechnical structures under lateral cyclic loading has attracted concerns from engineers (Achmus *et al.* 2009, Banerjee and Shirole 2014, Ma *et al.* 2018, Yan *et al.* 2021, Giannakos *et al.* 2012, Shi *et al.* 2018, Chen *et al.* 2020). In order to estimate the long-term deformation of geotechnical structures, cyclic tests were widely performed to obtain the surrounding soil's deformation characteristics. It has been accepted that soil's deformation depends on cyclic loading amplitude, initial deviatoric stress and loading directions (Wichtmann *et al.* 2005, Igoe and Gavin 2021, Nong *et al.* 2020, Pan *et al.* 2022). Numerical simulations have also been conducted to foresee the deformation of wharves or offshore structures subjected to lateral cyclic loading. For obtaining reasonable results, a suitable constitutive model is necessary to comprehend soil's deformation under lateral cyclic loading. Giannakos *et al.* (2012) used the constitutive model with kinematic hardening and associated plastic flow rule to simulate the reaction of piles that were fixed in sand. However, the model cannot consider the volumetric deformation of the soil and poorly predicts the pile-soil interaction.

Achmus *et al.* (2009) used a model to predict the deformation of piles under cyclic loading in sandy ground. Plastic strain accumulation was achieved by degrading the modulus of soil as the loading cycles increased. The input parameters for the model were calibrated using axial cyclic loading test results. However, Liu and Xue (2022) argued that the stress path of lateral cyclic loading differs significantly from that of axial cyclic loading as shown in Fig. 1. According to Wang *et al*. (2021a, b) and Xiong *et al*. (2016), the stress paths of cyclic loading have significant effects on the deformation of soils. This implies that soil may exhibit different deformation properties under lateral cyclic loading, as compared to axial cyclic loading. Therefore, the test results from lateral cyclic loading may be more credible than that from axial cyclic loading for better modelling of the cyclic response of geotechnical structures to wave or wind loading.

There is insufficient information available regarding the deformation characteristics of soils under lateral cyclic loading. Liu and Xue (2022) studied the deformation characteristics of a kaolin clay subjected to lateral cyclic

*Corresponding author, Research Professor
E-mail: zhiyongliu@tongji.edu.cn
[a]Ph.D.
[b]Ph.D. Student
[c]Ph.D.
[d]Ph.D. Student

Copyright © 2023 Techno-Press, Ltd.

ISSN: 2005-307X (Print), 2092-6219 (Online)

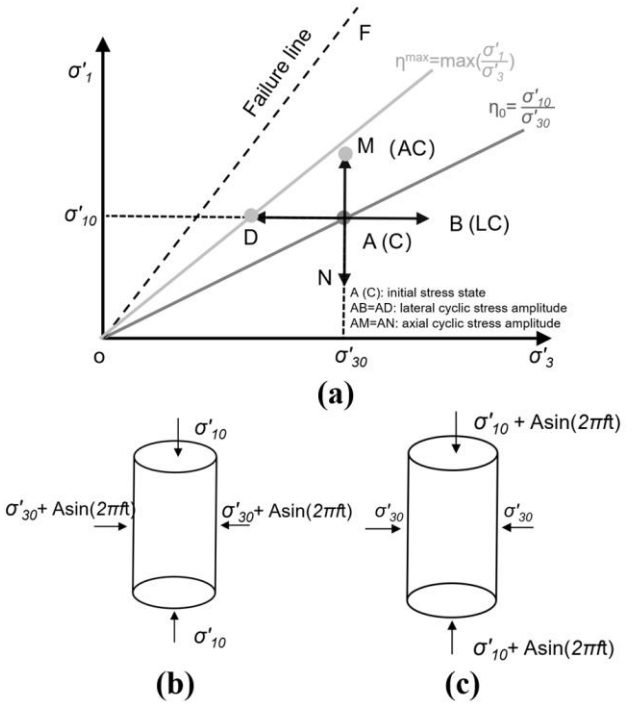

Fig. 1 (a): the stress paths under lateral (LC) and axial (AC) cyclic loading, (b): LC loading, and (c) AC loading; f is the loading frequency and *t* is time, the subscript of "0" in σ'_{30}, σ'_{10} means the initial stress state after consolidation

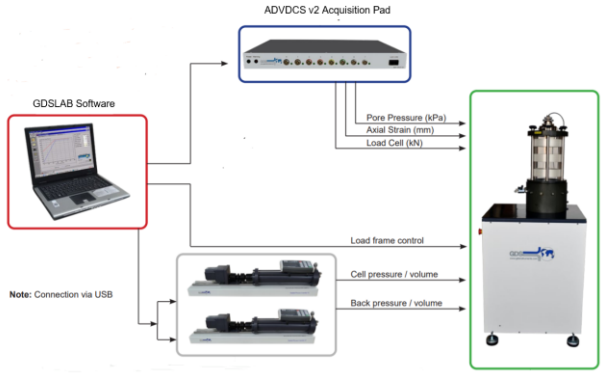

Fig. 2 The dynamic triaxial testing system

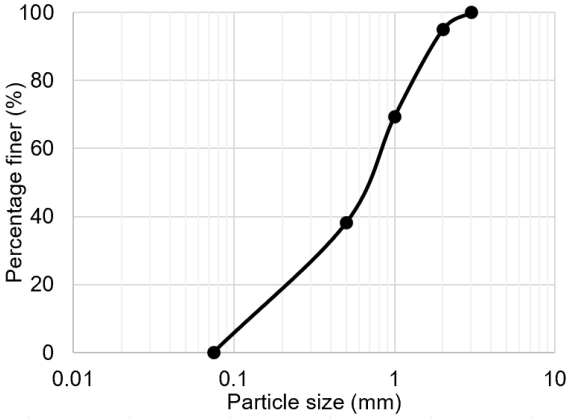

Fig. 3 The grain size distribution curve of the tested sand

loading under undrained conditions. According to the authors, lateral cyclic loading caused the buildup of plastic strain and excess pore water pressure (EPWP).

This study extends the work of Liu and Xue (2022) and aims to understand the deformation characteristics of sand under lateral cyclic loading. To achieve this, the cell pressure was cycled while maintaining a constant vertical stress. Strain accumulations are measured and analysed considering various initial stress ratios, lateral cyclic stress amplitudes and cyclic stress paths. The impact of cyclic loading direction on the deformation characteristics is identified and the flow direction is also investigated.

2. Soil and test detail

Cyclic tests were performed using a dynamic triaxial system which is shown in Fig. 2. The system can perform stress/displacement controlled cyclic tests with a maximum frequency of 5 Hz in the axial direction. The confining pressure can be also cycled under a low frequency using a confining pressure/volume controller manufactured by GDS Instruments Ltd., U.K. Detailed description about the testing system can be founded in the reference of Liu and Xue (2022).

Fujian standard sand was utilized as the material. It is a coarse quartz sand with subrounded particles. The physical properties are summarized in Table 1 and the grain size distribution curve is shown in Fig. 3. The samples were prepared using the air pluviation method. To achieve the uniformity, the sand was compacted by layer-to-layer and with five layers in total. The relative densities are 0.42-0.44 for all the samples. According to Liu *et al*. (2023), the sand has a peak friction angle of approximately 34° at the given relative density, and the stress-strain curve is shown in Fig. 4. All the samples are 50 mm in diameter and 105 mm in height. In order to achieve a Skempton's B-value greater than 0.95, the samples were subjected to carbon dioxide, de-aired water, and a back pressure of 400 kPa in succession. More details about the sample preparation and saturation are referred to Liu *et al.* (2021a, b).

After obtaining the targeted Skempton's B-value, the samples were consolidated to various initial stress ratios (η_0), the ratio of effective vertical (σ'_{10}) to lateral (σ'_{30}) stresses.

$$\eta_0 = \frac{\sigma'_{10}}{\sigma'_{30}} \tag{1}$$

The samples underwent isotropic consolidation to an effective confining pressure of 100 kPa, succeeded by anisotropic consolidation to attain effective axial stresses ranging from 100 kPa to 200 kPa, leading to η_0 values between 1.0 to 2.0. The initial deviatoric stress ($q_0=\sigma'_{10}-\sigma'_{30}$) varies from 0 kPa to 100 kPa. The axial loads were maintained for about half hour to complete the anisotropic consolidation.

After that, the lateral stress was sinusoidally cycled under drained conditions along the stress path of A-B-C-D

Table 1 The properties of the tested sand

Specific gravity, G_s	Mean grain size d_{50} (mm)	Uniformity coefficient, $C_u=d_{60}/d_{10}$	Maximum void ratio, e_{max}	Minimum void ratio, e_{min}	Peak friction angle*	Critical state friction angle
2.64	0.7	7.32	0.71	0.32	34°	31.5°

Note: Measured at the relative density of 0.42-0.44

Table 2 The arrangement of the tests

	σ'_{30} (kPa)	σ'_{10} (kPa)	η_0	q_0 (kPa)	A (kPa)	Relative density	Comments
L1	100	100	1.0	0	30	0.43	
L2	100	120	1.2	20	30	0.43	
L3	100	150	1.5	50	30	0.44	
L4	100	200	2.0	100	30	0.44	
L5	100	100	1.0	0	40	0.42	LC
L6	100	120	1.2	20	40	0.42	
L7	100	150	1.5	50	40	0.44	
L8	100	200	2.0	100	40	0.43	
L9	100	100	1.0	0	50	0.44	
A1	100	200	2.0	100	30	0.44	
A2	100	200	2.0	100	40	0.44	AC
A3	100	200	2.0	100	50	0.44	
A4	100	200	2.0	100	90	0.44	

Note: The subscript of "0" in σ'_{30}, σ'_{10}, q_0 means the initial stress state after consolidation; $q_0=\sigma'_{10}-\sigma'_{30}$; A refers to the cyclic stress amplitude; LC: lateral cyclic loading; AC: axial cyclic loading

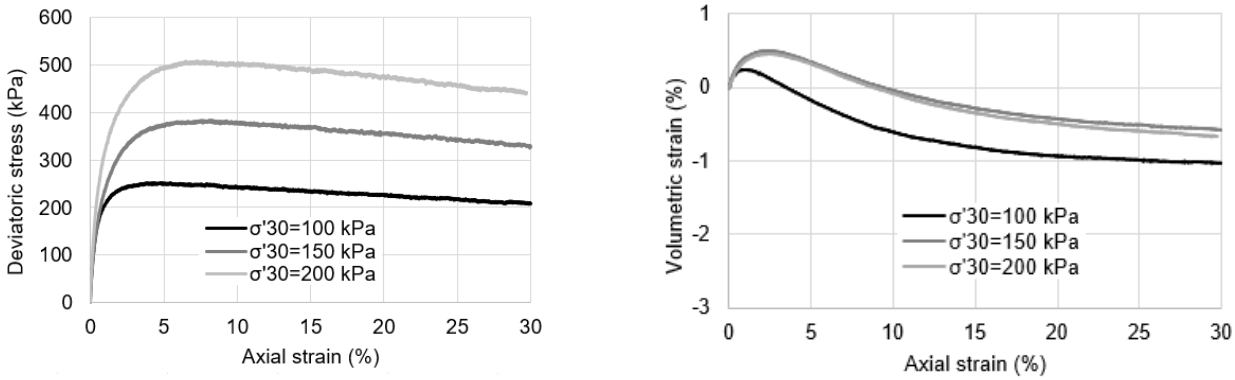

(a) The stress-strain curve (b) The volumetric-axial strain curve

Fig. 4 The behaviour of the sand under different confining pressures

in Fig. 1(a). The loading condition is shown in Fig. 1(b).

The lateral cyclic stress (A) varied from 30 kPa to 50 kPa. As suggested by Liu and Xue (2022), considering the capacity of the equipment, a frequency of 1/360 Hz was adopted, which is low enough to ensure a drained condition. For comparison, four samples were subjected to axial cyclic loading, corresponding to the stress path of A-M-C-N in Fig. 1(a) and the loading condition in Fig. 1(c) where the lateral stress was maintained constant. Each test was subjected to 70 loading cycles. The axial deformation was monitored using an encoder on the axial actuator and the volumetric deformation was measured using a back pressure/volume controller. The test arrangement is summarized in Table 2.

3. Results and discussions

This section reports the cyclic deformation of the sand subjected to different η_0 values, cyclic stress amplitudes and cyclic stress paths. The strain accumulations after 70 loading cycles are outlined in Table 3 where the positive axial and volumetric strains refer to compression in axial direction and contraction in volume, respectively.

3.1 Accumulated axial strain

3.1.1 Accumulated axial strain under lateral cyclic loading

Fig. 5 shows the stress-strain loops of the sand under

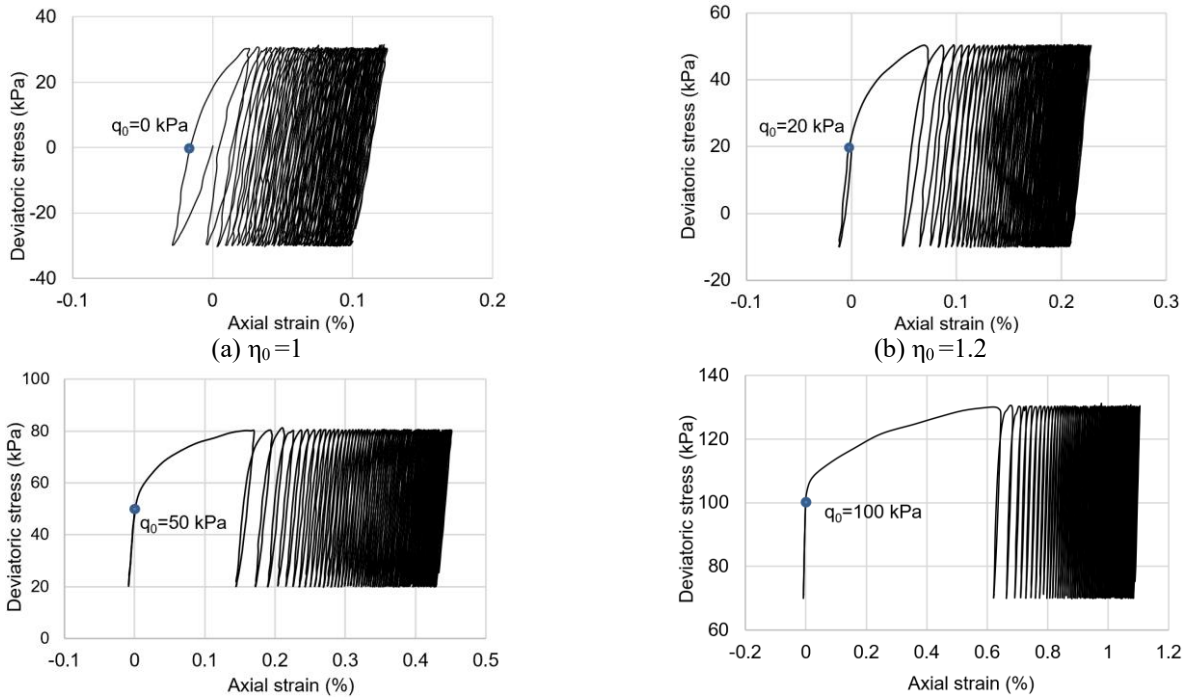

(a) η_0=1 (b) η_0=1.2

(c) η_0=1.5 (d) η_0=2

Fig. 5 The stress-strain loops of the sand under different η_0 values in lateral cyclic loading tests

lateral cyclic loading considering different η_0 values. The loops exhibit a similar trend wherein they expand considerably during the initial cycles and gradually contract thereafter. This indicates that the accumulation of plastic strain occurs significantly during the initial cycles and slows down gradually in the subsequent cycles, which can be better seen in Fig. 6.

In addition, under η_0 of 1.0, the samples are isotropically consolidated. The sample has been compressed in the axial direction as revealed in Figs. 5(a) and 6(c). This is different from that in clay where the sample experiences extension in the axial direction as shown in Fig. 7 under isotropic consolidation condition. This may be because of the changes in effective mean stress under different drainage conditions. The clay samples are under undrained cyclic shearing, so the effective mean stress decreases when EPWP builds up. This leads to rebound in the axial direction to some degree and axial tensile strain. In contrast, the sand samples are under drained conditions in the tests, so the volume reduces under the cyclic shear stresses. Therefore, the sand samples will undergo compression in the axial direction.

In addition, Fig. 5 indicates that the strain development during each cycle is affected by q_0, particularly in the first loading cycle. For instance, in the initial cyclic phase, the axial strain develops almost linearly with deviatoric stress and limited deformation is observed if the deviatoric stress is smaller than the initial deviatoric stress (q_0). However, the axial strain develops rapidly when the deviatoric stress is greater than q_0, suggesting a strong nonlinear behaviour of the soil. This means that the stress history or the initial deviatoric stress has noticeable influence on the soil's cyclic deformation behaviour.

Figs. 5 and 6 indicate that applying larger η_0 values results in greater strain accumulations and a greater η_0 value corresponds to a larger increment. For instance, when η_0 value shows a change of 0.5 from 1.0 to 1.5, the axial strain accumulation increases by only 0.33% from 0.11% to 0.44%. However, under the same increase in η_0 from 1.5 to 2.0, the accumulation increases by 0.66% from 0.44% to 1.1%. The similar effects of η_0 on the strain accumulations were also reported by Liu *et al.* (2021b). This is due to the nonlinear behaviour of the sand, as a greater η_0 value leads to a stress state closer to the soil's failure line. This will be further discussed later together with cyclic stress level.

Figs. 6(b) and 6(c) reveal the dependence of axial deformation on cyclic stress amplitude. Similar to axial cyclic loading, as shown in Table 3, increasing lateral cyclic stress leads to larger strain accumulation. This is also because the stress state in sand approaches closer to its failure line under greater cyclic stress magnitude, which is further discussed below together with the initial stress ratio.

As discussed earlier, increasing the initial stress ratio or cyclic stress enlarges axial strain accumulation. To better consider such effects, the maximum stress ratio (η^{max}) is calculated as the maximum ratio of the axial to lateral stresses during each cycle

$$\eta^{max} = \max\left(\frac{\sigma'_1}{\sigma'_3}\right) \tag{2}$$

The maximum stress ratio is affected by the initial stress ratio and cyclic stress amplitude, and is unchanged during a test.

Fig. 8 shows the relationship between the accumulated axial strain with η^{max} for all samples under different

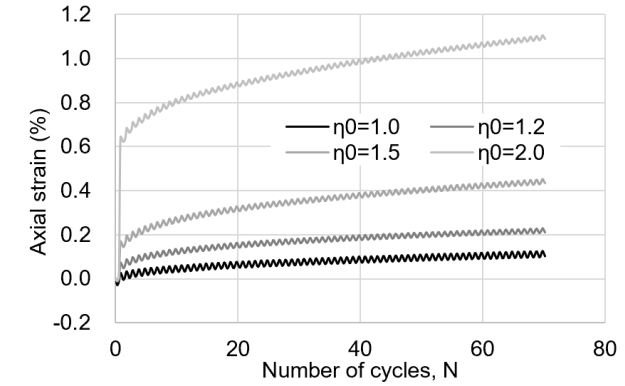

(a) A=30 kPa

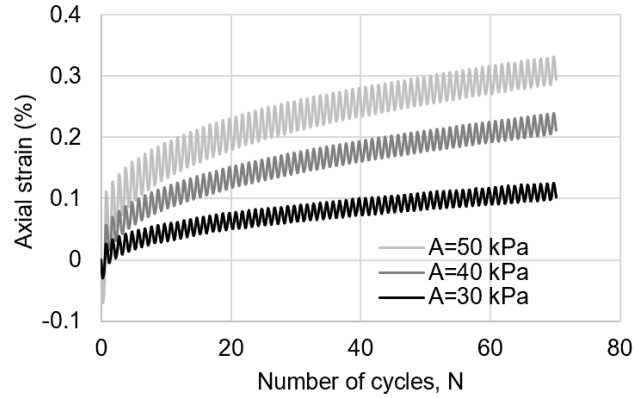

(b) η_0=1

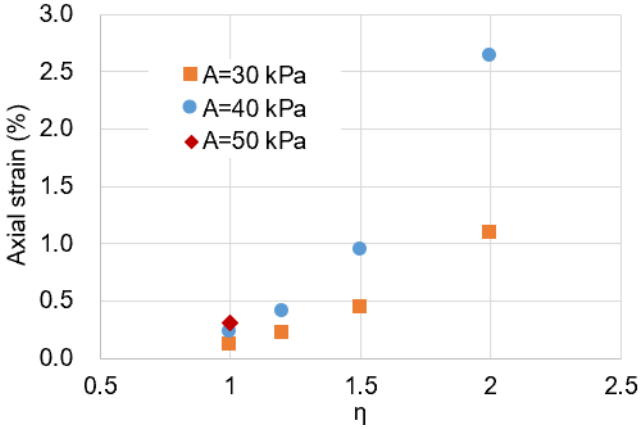

(c) The accumulated axial strain

Fig. 6 The accumulated axial strain under different testing conditions

conditions. Under lateral cyclic loading, even though the initial deviatoric stress and cyclic stress may be different, the accumulated axial strain always shows an exponential relationship with η^{max}. This implies that the impacts of initial static deviatoric stress and cyclic deviatoric stress on strain accumulation can be considered using the maximum stress ratio. This agrees with the finding by Chen *et al.* (2018) that the strain accumulation of soil under axial cyclic loading highly depends on the peak stress state and a greater maximum stress ratio results in greater strain accumulation.

This is because as claimed by Garcia-Rojo and Herrmann (2005), a greater maximum stress ratio leads to greater contact forces between particles and therefore a

Table 3 The drained cyclic test results

ID	η^{max}	ε_v^{acc} (%)	ε_1^{acc} (%)	ε_q^{acc} (%)
L1	1.43	0.30	0.11	0.01
L2	1.71	0.31	0.22	0.12
L3	2.14	0.26	0.44	0.35
L4	2.86	0.32	1.10	0.99
L5	1.67	0.40	0.23	0.09
L6	2.00	0.30	0.41	0.31
L7	2.50	0.51	0.94	0.77
L8	3.33	0.39	2.64	2.51
L9	2.00	0.71	0.31	0.08
A1	2.30	0.04	0.04	0.03
A2	2.40	0.05	0.08	0.06
A3	2.50	0.08	0.17	0.14
A4	2.90	0.33	0.48	0.37

Note: η_{max} refers to the maximum stress ratio during each cycle; ε_1^{acc}, ε_v^{acc} and ε_q^{acc} are the accumulated axial, volumetric and deviatoric strains, respectively, after 70 loading cycles

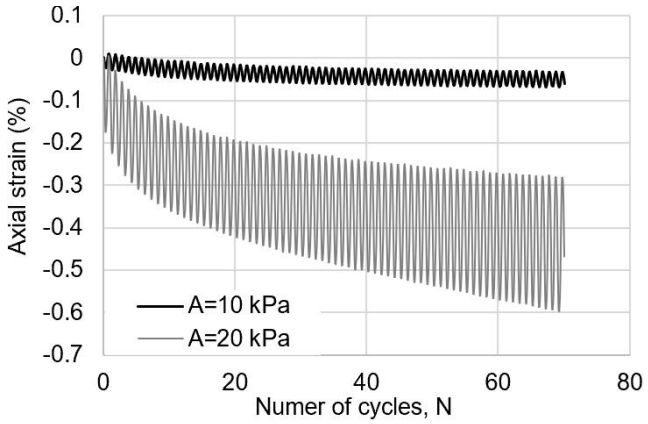

Fig. 7 The axial strain accumulation in an isotropically consolidated kaolin clay subjected to LC loading, data from Liu and Xue (2022)

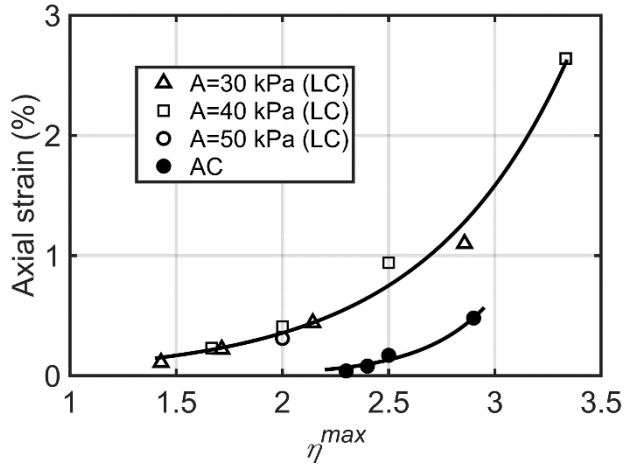

Fig. 8 The relationship between accumulated axial strain with the maximum stress ratio

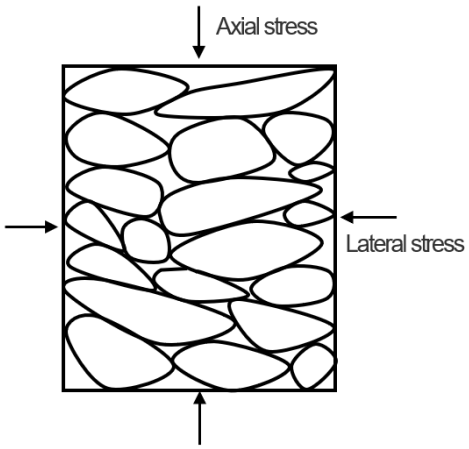

Fig. 9 The schematic diagram of the particle deposition

higher proportion of interparticle contacts in sliding which manifests as greater macroscopic deformations/strains.

Also, initial deviatoric stress has a similar influence with lateral cyclic stress magnitude on the axial strain accumulation. In other words, for the test with a greater initial stress ratio under smaller cyclic stress, axial strain accumulation could be comparable with that in the sample with a smaller initial stress ratio under greater cyclic stress if the maximum stress ratios are the same.

3.1.2 The internal anisotropy of the soil

As shown in Fig. 8 and Table 3, the samples subjected to lateral cyclic loading have greater axial strain accumulation than those under axial cyclic loading, even though the maximum stress ratio is the same. For example, under the maximum stress ratio of 2.5, there is an accumulation of approximately 0.94% in axial strain under lateral cyclic loading, while it is only about 0.17% under axial cyclic loading. This implies that the cyclic loading direction impacts the strain accumulation. A similar dependence of the deformation of sand on loading direction was also reported by Xiong *et al*. (2016). Such dependence is attributed to the internal anisotropy of soil. According to Yang *et al*. (2008) and as shown in Fig. 9, subrounded particles (the sand particles) display a preferred orientation of the long axis, with the direction being closer to the horizontal if the samples were prepared using the air pluviation method. The interlocking effect along the preferred direction of the long axis is relatively weaker compared to other directions, resulting in a lower strength of the sand in the horizontal direction as opposed to the vertical direction. Therefore, when the direction of cyclic loading is parallel to the preferred direction of the long axis (e.g., under lateral cyclic loading), greater strain accumulation could be observed than that under the direction of cyclic loading perpendicular to the long axis (e.g., under vertical cyclic loading). Such a phenomenon suggests that axial cyclic tests may underestimate the amount of sand deformation and lateral cyclic tests should be performed when predicting the response of geotechnical infrastructures subjected to wave, wind loading or other lateral cyclic loading.

3.2 Volumetric strain accumulation

Fig. 10 shows accumulated volumetric strain in the soil subjected to different testing conditions. Under different η_0 conditions, volumetric strain develops with loading cycles and the sand contracts. In addition, as shown in Figs. 10(a) and 10(c), unlike axial strain accumulation, the volumetric strain accumulations under different η_0 values are comparable, suggesting that it is minimally impacted by η_0 value. This supports the findings by Liu and Xue (2022) that under lateral cyclic loading, the buildup of EPWP in kaolin clay is little influenced by initial deviatoric stress as shown in Fig. 11. As revealed in the figure, EPWPs are almost the same under the initial stress ratios of 1.15-1.30, and slightly (about 3 kPa) smaller than that under the initial stress ratio of 1.0. Such a slight difference may be attributed to any test error.

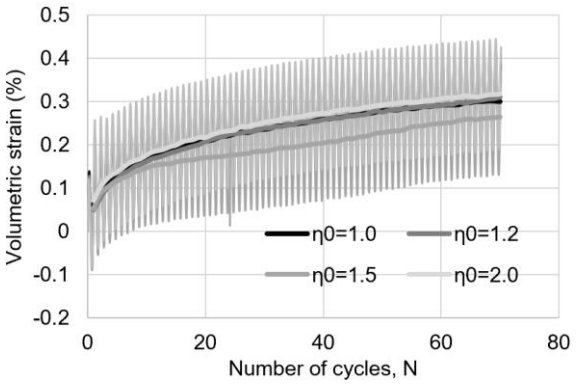

(a) A=30 kPa

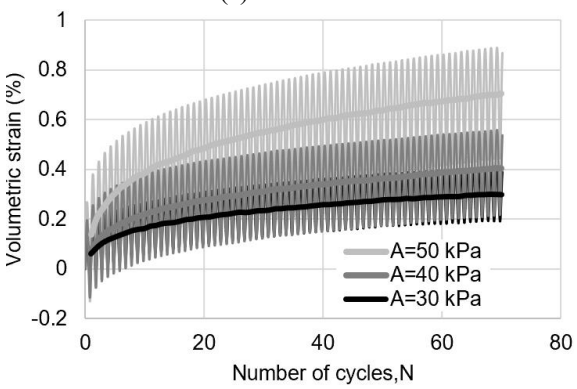

(b) η_0=1

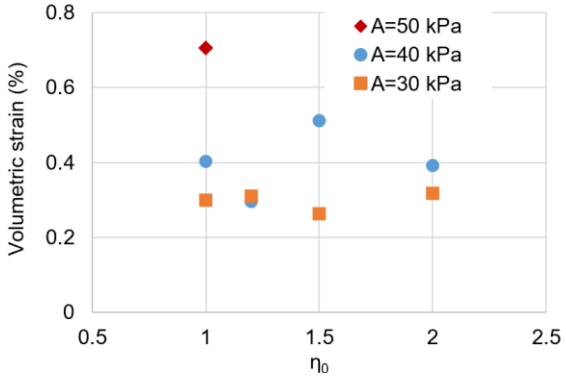

(c) The accumulated volumetric strain

Fig. 10 The accumulated volumetric strain under different testing conditions

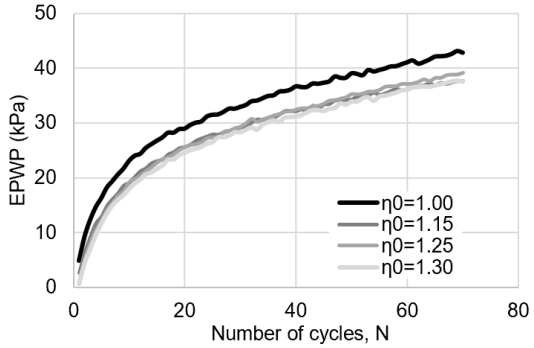

Fig. 11 EPWP in a kaolin clay exposed to LC loading under different η0 values, data from Liu and Xue (2022)

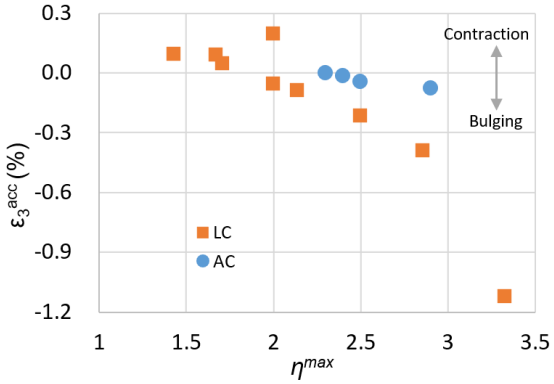

Fig. 12 The relationship between accumulated lateral strain with the maximum stress ratio

Figs. 10(b) and 10(c) show that there are noticeable impacts of cyclic stress levels on volumetric strain accumulation and increasing lateral cyclic stress causes greater volumetric strain accumulation. For example, when subjected to lateral cyclic stress of 30 kPa, there is an accumulation of approximately 0.3% in volumetric strain after 70 loading cycles while it is about 0.7% under the stress of 50 kPa. This is similar with that of the samples exposed to axial cyclic loading as shown in Table 3.

3.3 Discussions

During the tests, the axial (ε_1^{acc}) and volumetric (ε_v^{acc}) strain accumulations were measured. The lateral strain accumulation (ε_3^{acc}) can be calculated using Eq. (2)

$$\varepsilon_3^{acc} = \frac{\varepsilon_v^{acc} - \varepsilon_1^{acc}}{2} \tag{3}$$

In the equation, a negative ε_3^{acc} suggests the sample laterally bulging and a positive value means a contraction in the lateral direction. Fig. 12 reveals the calculated lateral strain in all the samples. The soil's lateral deformation varies from η^{max} and increasing the ratio could change the lateral deformation from contraction to bulging. For instance, the samples with η^{max} less than 2.0 undergo lateral contraction, and those with η^{max} greater than 2.0 experience bulging under lateral cyclic loading condition. In addition,

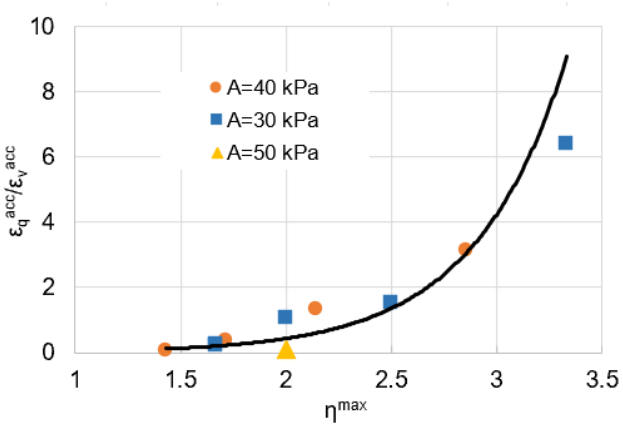

Fig. 13 The flow direction of the sand.

applying a greater η^{max} value results in greater lateral bulging deformation in the sand. For example, with η^{max} increasing from 2.5 to 3.33, the absolute value of lateral accumulated strain increases from 0.22% to 1.12%. Such phenomena suggest that the axial strain accumulation component increases with the maximum stress ratio in comparison to volumetric strain accumulation.

It is also found from Fig. 12 that even though η^{max} is the same, the samples subjected to lateral cyclic loading experience greater lateral bulging deformation when compared to those subjected to axial cyclic loading. For instance, with η^{max} of 2.5, the lateral strain is about 0.22% in the sample subjected to lateral cyclic loading while it is only approximately 0.04% under axial cyclic loading condition. This also implies that cyclic loading direction has great influence on the soil's deformation or the sand shows anisotropy.

According to Wichtmann *et al.* (2014), the deviatoric strain accumulation (ε_q^{acc}) is calculated using Eq. (3)

$$\varepsilon_q^{acc} = \varepsilon_1^{acc} - \frac{1}{3}\varepsilon_v^{acc} \tag{4}$$

Fig. 13 shows the relationship between the strain ratio ($\varepsilon_q^{acc} / \varepsilon_v^{acc}$) with the maximum stress ratio under lateral cyclic loading. Similar to the axial strain accumulation, there is an increase in strain ratio as the maximum stress ratio rises and a greater maximum stress ratio leads to a larger increment. In other words, as the maximum stress ratio increase, the deviatoric strain accumulation component increases compared with volumetric strain accumulation. For example, the strain ratio increases by 0.3 from about 0.1 to 0.4 if η^{max} increases from 1.5 to 2.0, while the increment is about 2.3 from 1.8 to 4.1 with the same increase in η^{max} from 2.5 to 3.0. This is consistent with the finding in Fig. 12. This means that with the increase of the stress ratio, the deviatoric strain could accumulate greatly with a little change in the soil volume at large η^{max} condition. In addition, even though the initial stress ratios and lateral cyclic loading levels are different, the flow direction always depends on the maximum stress ratio. This suggests that initial deviatoric stress has a comparable influence with lateral cyclic stress magnitude on the strain accumulation direction, which is similar to the axial strain accumulation.

4. Conclusions

A set of cyclic drained triaxial tests were performed to investigate the deformation behaviour of a saturated sand under either lateral or axial cyclic loading. The vertical stress was maintained, and the lateral stress was cycled to simulate the lateral cyclic loading. The impacts of initial stress ratio η_0, cyclic stress amplitude and cyclic stress path on the strain accumulations were presented and discussed. The deformation behaviour of the sand was compared with that of kaolin clay reported in the literature by the authors. For the limited number of tests, the following conclusions can be drawn:

(1) Applying lateral cyclic loading results in plastic strain accumulation in sand. The axial strain accumulation shows an exponential increase with the maximum stress ratio. In addition, the initial deviatoric stress has comparable effects with lateral cyclic stress amplitude on the accumulated axial strain. However, the accumulated volumetric strain increases with lateral cyclic stress magnitude but shows little dependence on the initial deviatoric stress, which is similar to the buildup of excess pore water pressure in clay subjected to lateral cyclic loading under undrained conditions.

(2) Though the maximum stress ratio is the same, lateral cyclic loading leads to greater axial and lateral bulging strain accumulations compared to axial cyclic loading. This means that the loading direction has effects on the strain accumulation or the sand shows anisotropy.

(3) The maximum stress ratio effects the soil's lateral deformation pattern and increasing the ratio could change the lateral deformation from contraction to bulging.

(4) As the maximum stress ratio increases, the deviatoric strain accumulation component increases compared with volumetric strain accumulation under lateral cyclic loading. This means that under large maximum stress ratio condition, the deviatoric strain could accumulate greatly with a little change in the soil volume. In addition, the initial deviatoric stress has a comparable influence with lateral cyclic stress magnitude on the strain accumulation direction.

According to Wichtmann et al. (2005) and Youd (1972), the strain accumulation of sand under drained cyclic loading shows independence on loading frequencies ranging from 0.05 Hz to 2 Hz. However, Nong and Park (2022) claimed that within the above range, loading frequency has noticeable effects on the volumetric strain accumulation of sand, and the higher the loading frequency, the smaller the strain accumulation. In this study, as recommended by Liu and Xue (2022), the cyclic loading was applied under a low frequency of 1/360 Hz with the consideration of the capacity of the equipment. It would be interesting to investigate the deformation behaviour of the sand subjected to lateral cyclic loading with higher loading frequencies. This would be achieved using a more advanced testing system in future studies.

Acknowledgements

The project is sponsored by Shanghai Sailing Program (No. 23YF1449100) and National Natural Science Foundation of China (No. U203420055).

References

Achmus, M., Kuo, Y.S. and Abdel, Rahman.K. (2009), "Behavior of monopile foundations under cyclic lateral load", *Comput. Geotech*., **36**(5), 725-735. https://doi.org/10.1016/j.compgeo.2008.12.003.

Banerjee, S. and Shirole, O.N. (2014), "Numerical analysis of piles under cyclic lateral load", *Indian Geotech. J.*, **44**, 436-448. https://doi.org/10.1007/s40098-013-0092-0.

Chen, X., Zhang, X., Zhang, Y., Ding, M. and Wang, Y. (2020), "Hysteretic behaviors of pile foundation for railway bridges in loess", *Geomech. Eng*., **20**(4), 323-331. https://doi.org/10.12989/gae.2020.20.4.323.

Chen, C., Zhou, Z.M., Kong, L.W., Zhang, X.W. and Yin, S. (2018), "Undrained dynamic behaviour of peaty organic soil under long-term cyclic loading, Part I: Experimental investigation", *Soil Dyn. Earthq. Eng*., **107**, 279-291. https://doi.org/10.1016/j.soildyn.2018.01.012.

Garcia-Rojo, R. and Herrmann, H.J. (2005), "Shakedown of unbound granular material", *Granular Matter*, **7**(2-3), 109-118. https://doi.org/10.1007/s10035-004-0186-6.

Giannakos, S., Gerolymos, N. and Gazetas, G. (2012), "Cyclic lateral response of piles in dry sand: finite element modeling and validation", *Comput. Geotech*., **44**, 116-131. https://doi.org/10.1016/j.compgeo.2012.03.013.

Igoe, D. and Gavin, K. (2021), "Investigation of cyclic loading of aged piles in sand", *J. Geotech. Geoenviron*., **147**(4), 04021011. https://orcid.org/0000-0003-3283-2947.

Liu, Z., Qian, J., Yaghoubi, M. and Xue, J. (2021a), "The effects of initial static deviatoric stress on liquefaction and pre-failure deformation characteristics of saturated sand under cyclic loading", *Soil Dyn. Earthq. Eng*., **140**, 106870. https://doi.org/10.1016/j.soildyn.2021.106870.

Liu, Z., Xue, J. and Ye, J. (2021b), "The effects of unloading on drained cyclic behaviour of Sydney sand", *Acta Geotech*., **16**, 2791-2804. https://doi.org/10.1007/s11440-021-01209-6.

Liu, Z. and Xue, J. (2022), "The deformation behaviour of an anisotropically consolidated kaolin clay under lateral cyclic loading", *Mar. Georesour. Geotec*., **40**(12), 1446-1452. https://doi.org/10.1080/1064119X.2021.2002986.

Liu, Z., Xiao, J., Xue, J. and Liu M. (2023), "The effects of changing the deviatoric and spherical stresses during cyclic loading on the drained response of a sand", *Can. Geotech. J*., Just-in. https://doi.org/10.1139/cgj-2022-0575

Ma, L., Wang, Y., Wang, W., Xu, X. and Li, S. (2018), "An analysis method for nearshore laterally loaded rigid pile in cohesive soil", *Mar. Georesour. Geotec*., **36**(1), 2-9. https://doi.org/10.1080/1064119X.2016.1255689.

Nong, Z., Park, S.S., Jeong, S.W. and Lee, D.E. (2020), "Effect of cyclic loading frequency on liquefaction prediction of sand", *Appl. Sci.*, **10**(13), 4502. https://doi.org/10.3390/app10134502.

Nong, Z. and Park, S.S. (2021), "Effect of loading frequency on volumetric strain accumulation and stiffness improvement in sand under drained cyclic direct simple shear tests", *J. Geotech. Geoenviron. Eng.*, **147**(12), 04021159. https://doi.org/10.1061/(ASCE)GT.1943-5606.

Pan, K., Xu, T., Liao, D. and Yang, Z. (2022), "Failure mechanisms of sand under asymmetrical cyclic loading conditions: experimental observation and constitutive modelling", *Géotechnique*, **72**(2), 162-175. https://doi.org/10.1680/jgeot.20.P.004.

Pan, K. and Yang, Z. (2018), "Effects of initial static shear on cyclic resistance and pore pressure generation of saturated sand", *Acta Geotech*., **13**(2), 473-487.

https://doi.org/10.1007/s11440-017-0614-5.
Qian, J., Li, S., Zhang, J., Jiang, J. and Wang, Q. (2019), "Effects of OCR on monotonic and cyclic behavior of reconstituted Shanghai silty clay", *Soil Dyn. Earthq. Eng*., **118**, 111-119. https://doi.org/10.1016/j.soildyn.2018.12.010.
Shi, J., Zhang, Y., Chen, L. and Fu, Z. (2018), "Response of a laterally loaded pile group due to cyclic loading in clay", *Geomech. Eng*., **16**(5), 463-469. https://doi.org/10.12989/gae.2018.16.5.463.
Wang, J., Wu, L., Cai, Y., Guo, L., Du, Y., Gou, C., Ni, J. and Gao, Z. (2021a), "Monotonic and cyclic characteristics of K0-Consolidated saturated soft clay under a stress path involving a variable confining pressure", *Acta Geotech*., **16**, 1161-1174. https://doi.org/10.1007/s11440-020-01031-6.
Wang, Y., Wan. Y., Ruan, H., Yu, X., Shao, J. and Ren, D. (2021b), "Pore pressure accumulation of anisotropically consolidated soft clay subjected to complex loads under different stress paths", *China Ocean Eng*., **35**(3), 465-474. https://doi.org/10.1007/s13344-021-0043-y.
Wichtmann, T., Niemunis, A. and Triantafyllidis, T. (2005), "Strain accumulation in sand due to cyclic loading: drained triaxial tests", *Soil Dyn. Earthq. Eng*., **25**(12), 967-979. https://doi.org/10.1016/j.soildyn.2005.02.022.
Wichtmann, T., Niemunis, A. and Triantafyllidis, T. (2014), "Flow rule in a high-cycle accumulation model backed by cyclic test data of 22 sands", *Acta Geotech*., **9**(4), 695-709. https://doi.org/10.1007/s11440-014-0302-7.
Xiong, H., Guo, L., Cai, Y. and Yang, Z. (2016), "Experimental study of drained anisotropy of granular soils involving rotation of principal stress direction", *Eur. J. Environ. Civ. En*., **20**(4), 431-454. https://doi.org/10.1080/19648189.2015.1039662.
Yan, Z., Zhang, H.Q., Xie, M.X. and Han, R.R. (2021), "Centrifuge bearing behaviors of batter-piled wharf under lateral cyclic loading", *Ocean Eng*., **226**, 108824. https://doi.org/10.1016/j.oceaneng.2021.108824.
Yang, Z., Li, X. and Yang, J. (2008), "Quantifying and modelling fabric anisotropy of granular soils", *Géotechnique*, **58**(4), 237-248. https://doi.org/10.1680/geot.2008.58.4.237.
Youd, T.L. (1972), "Compaction of sands by repeated shear straining", *J. Soil. Mech. Found. Div. ASCE* **98**(7), 709-725. https://doi.org/10.1061/JSFEAQ.0001762.

IC